C.E. SACLAY
DSM

DAPNIA/ 97-05 October 1997

FIRST BEAM TEST RESULTS WITH MICROMEGAS, A HIGH RATE, HIGH RESOLUTION DETECTOR

J. Derré, A. Giganon, Y. Giomataris, C. Kochowski, S. Loucatos, D. Jourde, G. Puill, Ph. Rebourgeard, J.P. Robert,

G. Charpak

DAPNIA

To appear in Nuclear Instruments & Methods in Physics Research A

Le DAPNIA (**D**épartement d'**A**strophysique, de physique des **P**articules, de physique **N**ucléaire et de l'**I**nstrumentation **A**ssociée) regroupe les activités du Service d'Astrophysique (SAp), du Département de Physique des Particules Elémentaires (DPhPE) et du Département de Physique Nucléaire (DPhN).

Adresse : DAPNIA, Bâtiment 141
CEA Saclay
F - 91191 Gif-sur-Yvette Cedex

DAPNIA–97–05
October 10, 1997

First beam test results with MICROMEGAS, a high rate, high resolution detector

J. Derré, A. Giganon, Y. Giomataris, C. Kochowski, S. Loucatos, D. Jourde, G. Puill, Ph. Rebourgeard, J.P. Robert

CEA/DSM/DAPNIA/C.E-Saclay
91191 Gif/Yvette, France

G. Charpak

CERN/LHC-EET, Geneva
and ESPCI, Paris

ABSTRACT

We present experimental tests, in particle beams, of a high rate, high position and time resolution gaseous detector, "MicroMegas", of $15 \times 15 cm^2$.

The rate capability is measured with 15 MeV protons from a TANDEM accelerator. No effect on gain is observed up to 10^9 particles/mm^2/s. With Argon and DME filling the gain is stable up to 50 mC total charge on a $3mm^2$ area.

With minimum ionizing particles in a CERN beam a high efficiency, close to 100%, was measured, under stable conditions.

A first measurement of space resolution of 50 μm $\pm$ 20 μm has been obtained.

The operation of the chamber shows that it is possible to optimize the geometrical parameters in order to improve the space resolution and bring the time resolution as low as to contain the events of each beam crossing (every 25 ns) in the European Large Hadron Collider. Further work is actively pursued in this direction.

1 Introduction

In order to sign interesting, rare events in future High Energy Physics investigations, the number of collisions and, therefore, the luminosity of the future accelerators must be pushed to highest values. For example, at the CERN Large Hadron Collider (LHC), the designed luminosity in excess of $10^{34}/\mathrm{cm}^2/\mathrm{s}$ with an inter-bunch crossing time of 25 ns, requires high speed, high granularity, radiation-hard tracking detectors. We present here tests of a new detector, MicroMegas , (MicroMesh Gaseous Structure) [1], meeting this challenge.

Silicon microstrip detectors are good candidates for their accuracy, but they suffer from radiation dammage induced by particles and especially heavily ionizing low-energy charged particles or neutrons, when the neutron flux is superior to 10^{13} neutrons/cm^2/year. The MSGC detector[2] is considered as an alternative to the multiwire proportional chamber. This new class of microstrip gaseous detectors can achieve a space resolution for minimum ionizing particles of 35 μm and its rate capability exceeds 10^6 particles/mm^2/s[3, 4]. These devices are, however, quite delicate for real operation in particle beams, presenting serious instabilities, mainly due to the presence of the insulating support in the region of the avalanche growth[5, 6].

MicroMegas , based on a novel double-stage parallel-plate avalanche configuration combines high space and time resolution, stability, simplicity and low cost. Several laboratory tests on a small prototype and preliminary simulations have shown excellent properties of this new detector; fast response, high gas gains superior to 10^4, fast (100 ns) ion space charge evacuation, excellent energy resolution and stable operation. The performance of this detector relies on the special field configuration and the narrow gap of 50 to 100 μm. Its quality relies on the simple techniques which have been developed for a good parallelism, for large surfaces, between an anode plate and a thin cathode grid of a few microns thickness, limiting the amplification gap. It relies also on a favorable situation, for large amplification factors, due to a compensating effect : when the gap decreases, the field increases but the number of ionizing collisions decreases. This limits the effect of gap defects or gas pressure variations. It plays certainly a fundamental role in allowing high gain operation beyond 10^5.

In this paper we present experimental results obtained with several MicroMegas prototypes having a $15 \times 15 cm^2$ active area.

2 Description of the detector and principle of operation

A detailed description of the detector can be found in [1]. It is a double stage parallel plate chamber, composed, as shown in figure 1, of a 3 mm conversion gap and a 100 μm amplification gap, separated by a micromesh. This is a metallic Nickel grid, 3 μm thick, made by electrodeposition technique. The typical optical transparency is about 50% and the step of the openings varies from 12 μm to several tens of μm. Most of the tests have been performed using a model having 37 μm openings every 50 μm. A negative voltage is applied on the migrogrid, which defines the cathode element of the

amplification gap. Golded copper anode strips, grounded through charge preamplifiers to define the anode potential, are printed by standard lithography on an epoxy plate or on a thin kapton foil. The standard epoxy used is 1.6 mm thick. Thinner ones (400 μm), commercially available, have also been tested. The thickness of the copper is 9 μm on both sides of the epoxy. In order to counterbalance the stretch of the material a grid-like pattern was printed on the back face. We have used also a kapton support of 25 μm thickness and a copper thickness of 4 μm. Anode strips have a pitch of 317 μm and are separated by 70 μm gaps. The uniformity of the amplification gap is maintained by using precise insulating spacers between anode and cathode plane. We have used two different spacer techniques. One consists of quartz fibers, 4 mm spaced, 100 μm in diameter, glued on the epoxy orthogonally to the anode strips. The microgrid is softly stretched on a G10 frame lying on the fiber plane. The total active area is $15 \times 15 cm^2$. The third (drift) electrode is defined by a thin aluminized mylar streched on a G10 frame. The second spacer technique consists of cylindrical insulating pillars, 2 mm spaced, 100 μm thick, 200 μm in diameter, printed by standard lithography.

In a typical operation the high voltage on the grid is about 350 to 450 Volts defining a uniform high electric field of about 45kV/cm. The electric field in the drift volume can vary from a few hundred V/cm to several kV/cm.

Figure 1 shows a schematic view of the detector. A charged particle traversing the detector leaves in the gas a trail of electrons that drift in the conversion gap through the action of the weak electric field. They are transported through the microgrid into the amplification gap, where they are multiplied under the action of the high electric field. An avalanche of electrons is produced which is collected on the anode strips, while the ion cloud drifts in the opposite direction. As explained in [1], due to diffusion processes and the configuration of the electric field around the holes of the microgrid, the major part of these ions are quickly collected by the microgrid (100 ns). The fast ion collection has several benefits for the operation of the detector; the rise of the ion induction signal is fast, allowing confortable and fast signals at moderate gains and rapid evacuation of the space charge, permitting high counting rates.

3 Laboratory tests

Various tests are continuously being carried in the laboratory, following those presented in [1]. Several gas fillings have been tested, the most promising being Argon-dimethylether (DME) mixture, because of the low diffusion coefficient and low polymerisation compared to hydrocarbon quenching components. Excellent results, in terms of gain and stability, are obtained by adding a small fraction, up to 20%, of CF4 to the previous mixtures. In the latter case, the drift velocity can double, a great advantage for very high rate detector operation.

4 Beam tests

In the following sections we describe experimental results obtained with $15 \times 15 cm^2$ MicroMegas detectors at two particle accelerators.

i) An intense low energy proton beam (15 MeV) in the Saclay TANDEM, was used to investigate the counting rate capability of the detector.
ii) A high energy pion beam (10 GeV), the CERN-PS T9 beam, was used to study the performance of MicroMegas with minimum ionizing particles.

4.1 Tests at the Saclay TANDEM

We have carried out beam tests of a single detector at the Saclay TANDEM facility. This is a Van de Graaf accelerator, which can provide an intense proton beam with kinetic energy up to 20 MeV. The beam intensity can be tuned from 5 to 500 nA. Protons are scattered in the thin exit window 25 μm Kapton-foil. Therefore one can further adjust the beam intensity on the detector by moving the detector on a circle in the beam plane at various angles from the beam line. The set-up, shown in figure 2, consisted of a standard $15 \times 15cm^2$ MicroMegas detector with a 100 μm amplification gap with fiber spacers. The gas filling was a mixture of Argon with DME (Dimethyl-ether) or Isobutane. A 2 mm thick Cu plate was mounted in front of the detector with a small, 1 mm diameter, hole at the middle of the detector. The purpose of this plate is to dump the incident beam, leaving just a small passage for protons. The beam diameter projected at the detection surface of MicroMegas has been measured to be 2 mm. Two charge preamplifiers were used to detect the signals from the microgrid and from an ensemble of 40 strips interconnected and centered at the middle of the beam hole. The total surface of these 40 strips was sufficient to fully contain the proton beam.

The hole was placed at a known angle θ (θ= 5° for the first investigation) from the beam line at a given distance from the beam exit window. A scintillator (PM_1) counter was placed behind the chamber to measure the beam intensity when MicroMegas was removed. A second scintillator (PM_2) was placed on the other side of the beam line to monitor the beam intensity when MicroMegas was back in the beam. Indeed, the low energy proton beam passing through the collimator and reaching the MicroMegas entrance, was absorbed by the epoxy back-plane of the detector and only a small fraction could reach the first scintillator. A good linearity has been mesured between PM_1 and PM_2, allowing a precise evaluation of the beam intensity and therefore of the proton flux, taking into account the beam projection area at the detector.

First tests were performed by studying the detector signal through a discriminator-scaler or by reading out the corresponding charge using a charge sensitive ADC. The charge collected in the strip amplifier is shown in Figure 3. The distribution has a Landau shape and its most probable value, well separated from the pedestal, indicates a good detection efficiency. The gas filling was a mixture of Ar+5% Isobutane and the applied high voltages were 280 Volts on the microgrid (HV2) and 500 Volts on the drift electrode (HV1). Varying the beam intensity, we were able to study the behaviour of the signal of the detector coming out on the microgrid, up to about 10^6 protons/s, corresponding to a total particle flux of 3.10^5 particles/mm^2/s. A good linearity has been observed between the detector rate and the monitor rate in PM_2. The result demonstrates the stability of the detector at the above fluxes. This is confirmed by the charge distribution in the ADC, which remained stable. So, having observed no effect on either counting or gain of the detector, we moved the detector close to the beam line to increase the proton flux.

The detector was placed at θ=2°. Because of the slow electronics used, when the particle counting was not possible any more we used a standard electrometer to read the continuous current from the 40 interconnected anodes. The sensitivity of the electrometer was better than 1 picoAmpère, but during the measurement the electronic noise was about 500 pA because of the electrical connection to the detector. With this sensitivity we were able to measure the detector current in the ionisation mode, for particle intensities beyond 10^6 protons/s. Indeed, taking into account the total calculated deposited charge in the 3 mm conversion gap (1800 electron-ion pairs for 15 MeV protons) the corresponding current (3 nA at a flux of 3×10^6 particles/mm^2/s) was within the sensitivity of our measurement. Measuring the current in the ionisation mode is a precise and safe way to evaluate the gain of the detector; by increasing the amplification voltage the gain increases and its exact value is directly measured by comparing the current with the one measured in the ionisation mode (gain=1). Figure 4 shows the measured current as a function of the high voltage HV2, for various particle fluxes up to 2×10^7 particles/mm^2/s. A good linearity of all these curves is observed, so again we do not observe any saturation.

The detector was then placed in the beam line (θ=0°) and another mixture of Argon and DME was used to improve the radiation resistance of the detector. Figures 5 and 6 show current curves as function of HV2, at various particle fluxes, for Ar+5% DME and Ar + 20% DME. Again, the linearity is good, there is no sign of saturation due to space charge. We observed a decrease of the maximum charge per avalanche with increasing particle flux; at the highest flux (Figure 6) the total charge per avalanche was limited to about 50000 electrons. This effect is attributed to the tail of the Landau fluctuation producing large avalanches in the detector, leading to an excess of the spark intensity. The number of sparks, proportional to the particle flux, can limit the maximum gain of the detector at very high fluxes. Another reason is that during these investigations performed at very high particle fluxes we observed a degradation of the detector; due to the high current, cathode strips were heated-up and the golded protection layer was locally removed, creating a limitation of the maximum gain of the detector.

A fast investigation was peformed, in these last conditions, to test the radiation resistance of the detector. The beam intensity was at its maximum value, giving a current in the detector of 10 μA. The detector current was monitored for 80 minutes (the additional beam time allocated before the definitive TANDEM shutdown...) The high voltage applied on the microgrid was HV2 = 320 Volts and the gas mixture Ar + 20% DME. As is shown in Figure 7 the current was stable during this measurement. Integrating the total charge accumulated in the detector we find Q=50 mC on the 3 mm^2 irradiated area. It corresponds to about 10 years for a detector located at 40 cm from the beam pipe of the LHC collider, running at its full luminosity.

4.2 Results in a CERN particle beam

The apparatus was installed in the CERN-PS beam line providing a negative pion beam of 10 GeV/c. It consisted of two "standard" MicroMegas chambers with horizontal strips mounted close to each other between two drift chambers and scintillation trigger counters.

The MicroMegas read-out electronics consisted of charge preamplifiers having 2000

electrons RMS noise and 1.5 Volts/pC sensitivity. A group of 24 strips in the central part of the first detector and only a group of 6 strips of the second detector was equipped with these electronics. Signals were brought through 30 m BNC cables to LeCroy 2249A ADCs read out through CAMAC driven by a MacIntosh computer.

The two drift chambers were each equipped with x–y planes, each plane containing six cells of 2.5 cm drift space between a double sense wire and a single cathode wire, flushed with a standard gas mixture of Ar + 30% Isobutane. The two chambers were placed at 2 m distance each from the MicroMegas doublet, one upstream and one downstream. They had a space resolution of about 150 μm. Double tracks in the same cell were not resolved.

4.2.1 Track selection

Using the two drift chambers, tracks are recognized and their trajectory reconstructed within 100 μrad. Reconstructed tracks are pointed to the MicroMegas plane and only those passing inside the read-out zone of the detector are selected. We select straight, single tracks reconstructed in the two drift chambers and in the second MicroMegas . In this way we reject tracks which are badly reconstructed, for instance due to pile-up of two tracks, or due to other effects like large multiple scattering or nuclear interactions.

4.2.2 Cluster size

A simple cluster finding algorithm is used to identify the group of strips fired, each beyond 4σ of its pedestal, at each passage of a charged particle through MicroMegas . The strip multiplicity is shown in Figure 8 for various gas mixtures Ar + 2% Isobutane (a), Ar+ 4% Isobutane (b) and Ar+ 7% Isobutane (c). The strip multiplicity decreases by adding Isobutane. Monte Carlo simulations confirming such behaviour, show that the strip multiplicity is dominated by the electron diffusion process in the conversion-drift gap. Using a low diffusion gas like the DME one can obtain lower strip multiplicity. Figure 9 shows the transverse diffusion as a function of the electric field, expected from Monte Carlo simulation, for Argon and 10% DME gas mixture. Transverse diffusion exhibits a maximum at 1.5 kV/cm for that mixture. This property, predicted from simulation, was verified experimentally in the laboratory:in the same figure the second curve shows the strip multiplicity observed in MicroMegas for the same gas mixture during irradiation of the detector with 5.9 KeV X-rays. It shows an increase between 200 V/cm and 1.5 kV/cm, as it is expected from the simulation.

4.2.3 Efficiency

The detection efficiency is evaluated by counting the percentage of events with a cluster in the first MicroMegas for a track identified by the two drift chambers and confirmed by the second MicroMegas chamber.

The efficiency as a function of the applied voltage (HV2) on the micromesh is shown in Figure 10 for various gas mixtures. It reaches a high value of 99.5 % and the plateau is quite large taking into account that the cut-off applied on the collection

charge corresponds to 8000 e^-/strip. A careful design of the electronic connection would permit to decrease the noise to its nominal value (1000 electrons) and widen the plateau.

A study has been performed to investigate the uniformity of the efficiency over the active surface of the detector. Figure 11 shows the beam profile in the horizontal view (along the detector strips), using the two drift chambers, for events giving no signal in the detector. We observe a concentration of the inefficiency in small bands, which correspond to the fiber spacer positions. The conclusion is that only a small loss of the efficiency has been observed, due to the fiber spacers. Outside this area the efficiency is total.

4.2.4 Space resolution

In this set-up it is difficult to measure the space resolution of MicroMegas . Pointing the tracks, reconstructed by the two DCs, to the detector plane, the intercept point has a poor resolution due to the drift chamber resolution and the multiple scattering effect. The telescope resolution is roughly estimated to be $155 \pm 5 \mu m$. The difference between this point and the centroid in MicroMegas , as shown in Figure 12 is a convolution of the resolution of the intercept point and the detector resolution. It is largely dominated by the drift chamber resolution. Deconvoluting the two numbers we can give a first estimate of the MicroMegas resolution of $50 \pm 20 \mu m$ for a mixture of Argon with 7 % Isobutane. Changing the gas mixture we find $60 \pm 15 \mu m$ and $105 \pm 10 \mu m$ for 4 % and 2 % Isobutane respectively. This estimate is only an upper limit. Recent tests (see next section), show that the resolution of this MicroMegas prototype is close to 40 μm. Monte Carlo simulations indicate that by choosing an appropriate pitch and low diffusion gas one can achieve an accuracy better than 20 μm. A detailed analysis is under way and will be presented in a coming publication.

5 Current and future developments

We are pursuing the research to optimize the gas mixtures suitable for minimum ionising particle detection with respect to ionisation density, transverse diffusion and space resolution, aging properties, detector stability and maximum gas gain. A high current (50 mA) x-ray generator, with copper cathode, is being used for systematic investigations of high flux behaviour of the detector and for a detailed study of the radiation resistance of the detector at different gas conditions. Indeed, the slow aging of the parallel plate gas chambers allows the use of a variety of gas mixtures aiming at the optimization of the detector, in terms of time resolution, space resolution, two-track resolution, operation in a magnetic field, maximum particle flux, presence of heavy ionising particles, neutrons etc.

The measurement of the space resolution of the detector is an important task. It is known that an analogue microstrip read-out allows a good localisation of the avalanche position using the centroid of the strip signals. Results and perspectives on this topic were mentioned in the previous section. We pursue the work developing narrower strips in order to study the limits of the accuracy of this detector.

Large size detectors have a wide field of applications in high energy physics and other domains. Using present technology, detectors of $50 \times 50 cm^2$ will be constructed in the near future. Concerning larger size detectors, printed circuits bearing anode strips are available, but microgrids commercially available are limited in size. One solution is to mount, on a large printed circuit, a mosaic of several microgrids in order to cover the total surface. As an example, 4×4 =16 such elements glued on a insulating border of 3 mm, will define a dead space of about 4%, acceptable for some experiments. A second solution is the development of large size microgrids, which simplifies the construction of large detectors, but their behaviour at high rate must be tested, as well as the resistance to sparking.

The high efficiency measured shows that the conversion space could be reduced by at least a factor of two without significant loss of the efficiency. Reduction of the conversion space brings on a great benefit, since the time dispersion becomes smaller, the degradation of the space resolution, due to inclined tracks is lower and the effect of the magnetic field decreases. We started constructing detectors with small conversion space and measuring their efficiency.

5.1 New beam tests

The results presented above have been obtained from tests run in 1996.

A battery of 5 detectors was tested during 1997. The goal was to improve the accuracy and the efficiency, in order to define the optimum thickness of the conversion gap and reduce the occupation time of the chamber, due to the drift of electrons and ions, to a minimum value, within the period (25 ns) of a beam crossing of the LHC. For some specific, high rate experiments like the new fixed target experiment, COMPASS [7], recently approved by the SPS committee, the chamber was tested using fast preamplifiers (type MQS 104 Lecroy) and data is under analysis.

In the summer of 1997 two MicroMegas chambers were tested in a magnetic field, inside a spectrometer set-up containing several tracking detectors of different types. This prototype spectrometer was assembled in order to estimate the performance of a future neutrino oscillation detector with high tracking and vertexing resolution. It originated from a common effort of NOMAD and CHORUS teams, aiming to a new generation detector, upgrading the performances of these two experiments [8]. The efficiency of MicroMegas inside the 1.3 T magnetic field, the correction of the Lorenz angle and the resolution using information from the other trackers have been measured and will be presented in a future publication.

6 Applications

Most of the applications of the novel detector rely on new features which are, in summary :

1. High granularity can be obtained in a straightforward fashion. Metallic strips of a large variety of pitches can be printed using conventional low-cost lithography

on a epoxy or thin kapton substrate. One can produce strips of any shape, since the operation of the detector is independent of the strip shape. This can open the way to build detectors having detection elements other than straight strips: pads, circular strips, variable pitch elements etc.

2. Low thickness material : there is no obstacle to reduce the total material of the detector at the level of the MWPC radiation lenght. By using a Kapton thin foil as the strip substrate the total material will not exceed 10% of a typical silicon strip detector.

3. High counting rate : thanks to the fast evacuation of positive ions in less than 100 ns and the special electric field configuration, its rate capability exceeds by several orders of magnitude conventional detectors. First results indicate that a counting rate up to 10^9 particles/mm^2/s can be obtained.

4. Stable operation and excellent aging behaviour of the detector, as observed

5. Low cost : the construction of the detector is achieved using known-low-cost technology.

The most important applications of MicroMegas are in High Energy Physics experiments, especially in the future high luminosity projects at the LHC.

Of particular interest is the CMS detector[10], which is planning to use massively gaseous microstrip detectors, therefore the employment of MicroMegas can improve the tracking system and reduce at the same time the total cost.

As mentioned above, a study is actually under progress to use MicroMegas for the tracking system of COMPASS. Its use is justified by the high muon flux in the very-forward region, which can reach 10^6 particles/mm^2/s. A particular effort is invested to optimize fast electronic read-out. As mentioned, beam tests are under way.

Another candidate is the planned upgrade of the NOMAD/CHORUS detector [8].

Beyond particle physics many new fields of research are now opened by the exceptional caracteristics of MicroMegas : the combination with secondary electron emmitters in order to reach subnanosecond time resolution, the combination with high efficiency X or gamma ray converters, which can lead to major advances in radiography.

7 Conclusions

The operation of several MicroMegas prototypes set up in various beam conditions has shed light on the rate capability, the long-term stability, the space resolution and the efficiency for minimum ionising particles of this detector.

- With heavily ionizing particles (15 MeV protons) the detector was able to operate at very high fluxes, up to 2×10^9 particles/mm^2/s without saturation of the amplification factor. We have found it is possible to work under conditions of total protection of the detector and of the electronics from occasional sparks.

- Preliminary radiation dammage tests have shown a rather good resistance of the detector. They have been performed at very high particle rate. Further detailed tests are in preparation to measure the radiation resistance of the detector.

- Full efficiency for minimum ionising particles has been measured in a particle beam with a 3 mm conversion gap. This opens the way towards thinner detectors, with about 1 mm gaps, in order to improve the time and space resolution of inclined tracks.

- A first investigation of the space resolution shows that one can achieve a precision of about 50 μm with strip pitch of 317 μm. It is limited by the diffusion coefficient of the gas mixture and strip width. Better resolution can be obtained by using gases having lower diffusion coefficient and narrow anode strips.

Acknowledgements

We thank R. Veenhov for developments of GARFIELD[11] code specific to Micro-Megas , and Ph. Briet for the printed circuit designs.

References

[1] Y. Giomataris, Ph. Rebourgeard, J.P. Robert and G. Charpak Nucl. Instr. Meth. A376(1996)29-35.

[2] A. Oed, Nucl. Instr. Meth. A263(1988)351

[3] F. Angelini, R. Bellazzini, A. Brez, M.M. Massai, G. Spandre and M.R. Torquati, Nucl. Instr. Meth. A283(1989)69

[4] R. Bouclier, J.J. Florent, J. Gauden, G. Million, A. Pasta, L. Ropelewski, F. Sauli and L. I Shekhtman, Nucl. Instr. Meth. A323(1992)236.

[5] R. Bouclier, et al., Presented at the IEEE 1996 Nuclear Science Symposium and Medical Imaging Conference Anaheim, November 3-9, 1996.

[6] V. Peskov, B.D. Ramsey and P. Fonte, Int. Conf. on Position Sensitive Detectors (Manchester, 9-13 Sept. 1996).

[7] CERN/SPSLC 96-14 SPLSLC/P297 and CERN/SPSLC 96-30 SPLSLC/P297 add.1.

[8] J.J. Gomez-Cadenas and J.A. Hernando, CERN-PPE/96-69.

[9] Results from beam tests, to be published.

[10] CMS Letter of intent, CERN/LHCC 92-3,1992

[11] GARFIELD CERN program library W5050

Figure Captions

Figure 1. A schematic view of MicroMegas (not to scale) : the 3 mm conversion gap is between the cathode electrode and the micromesh and the 100 μm amplification gap is defined by the micromesh and the anode strip electrode.

Figure 2. The set-up used for the TANDEM test. The proton beam is diffused on the target (thin mylar window). A collimator, a MicroMegas detector and a scintillator (PM1) are aligned an angle θ. A second scintillator (PM2) at large angle is the beam monitor.

Figure 3. The Landau energy loss distribution obtained with 15 MeV protons. The pedestal is at zero. High Voltage settings were HV1=500 Volts for the drift voltage and HV2=280 Volts for the micromesh voltage. The gas mixture was Ar+5% Isobutane.

Figure 4. Detector current versus HV2 for particle fluxes up to 2×10^7 particles/mm^2/s. HV1=500 Volts and gas mixture Ar+5% Isobutane.

Figure 5. Detector current versus HV2 for particle fluxes up to 4×10^8 particles/mm^2/s. HV1=400 Volts and gas mixture Ar+5% DME.

Figure 6. Detector current versus HV2 for particle fluxes up to 2×10^9 particles/mm^2/s. HV1=400 Volts and gas mixture Ar+20% DME.

Figure 7. Detector current versus time, for a gas mixture of Ar+20% DME. HV1=400 and HV2=320 Volts.

Figure 8. Strip multiplicity for various gas mixtures.

Figure 9. Transverse diffusion coefficient versus electric field for Ar +10% DME. In the same figure is plotted the measured strip multiplicity versus electric field in the conversion gap for the same gas mixture.

Figure 10. Detector efficiency versus microgrid high voltage HV2, for various gas mixtures; a) Ar+2% Isobutane, b) Ar+4% Isobutane.

Figure 11. Beam profile of particles giving no signal in MicroMegas . The observed peaks (inefficiency) are due to the fiber spacers.

Figure 12. The residual distance between the reconstructed track and the centroid in MicroMegas , for various gas mixtures; Ar + 2% Isobutane, Ar + 4% Isobutane, Ar + 7% Isobutane.

MICROMEGAS

Micro Mesh Gaseous Structure

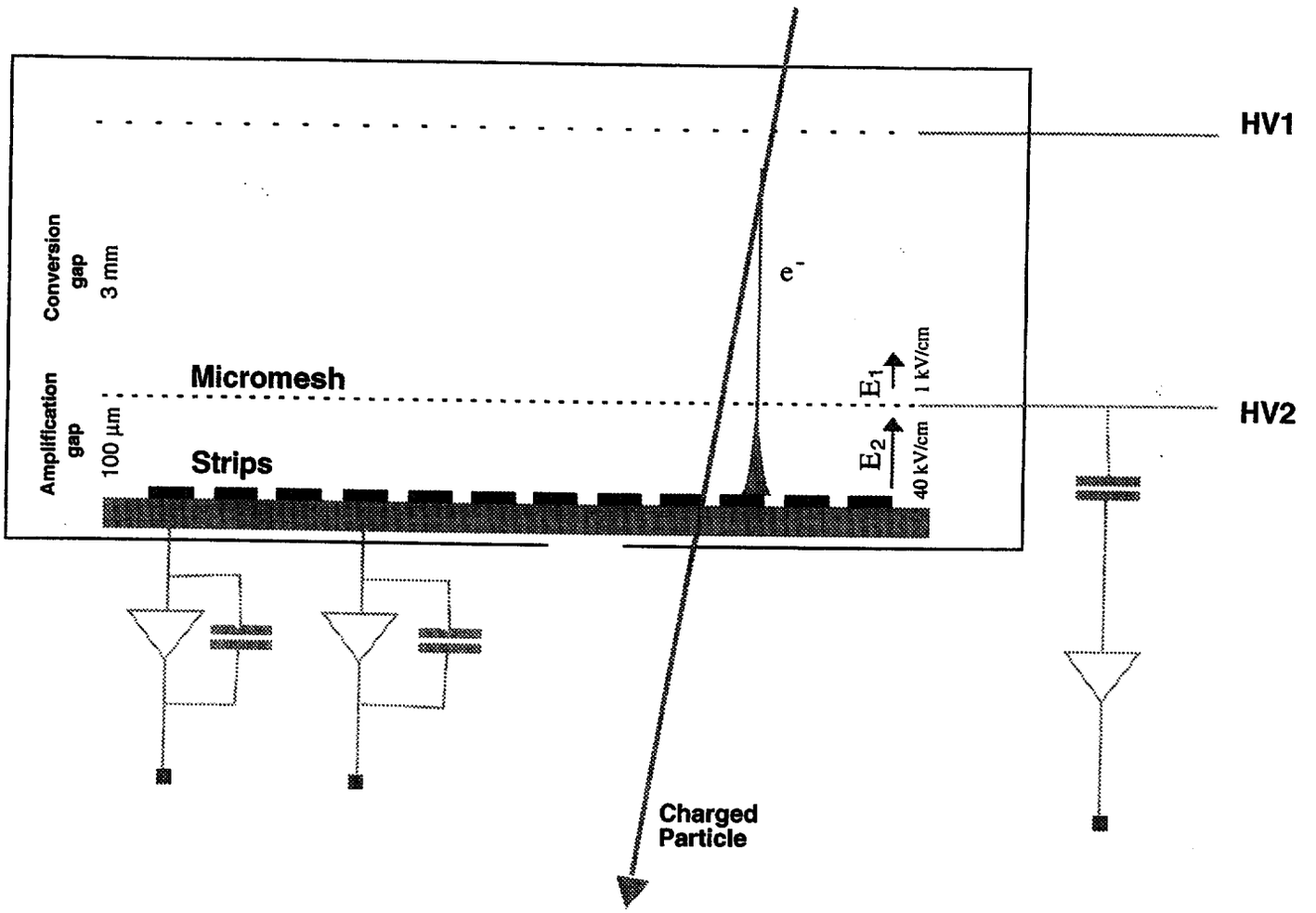

Fig. 1

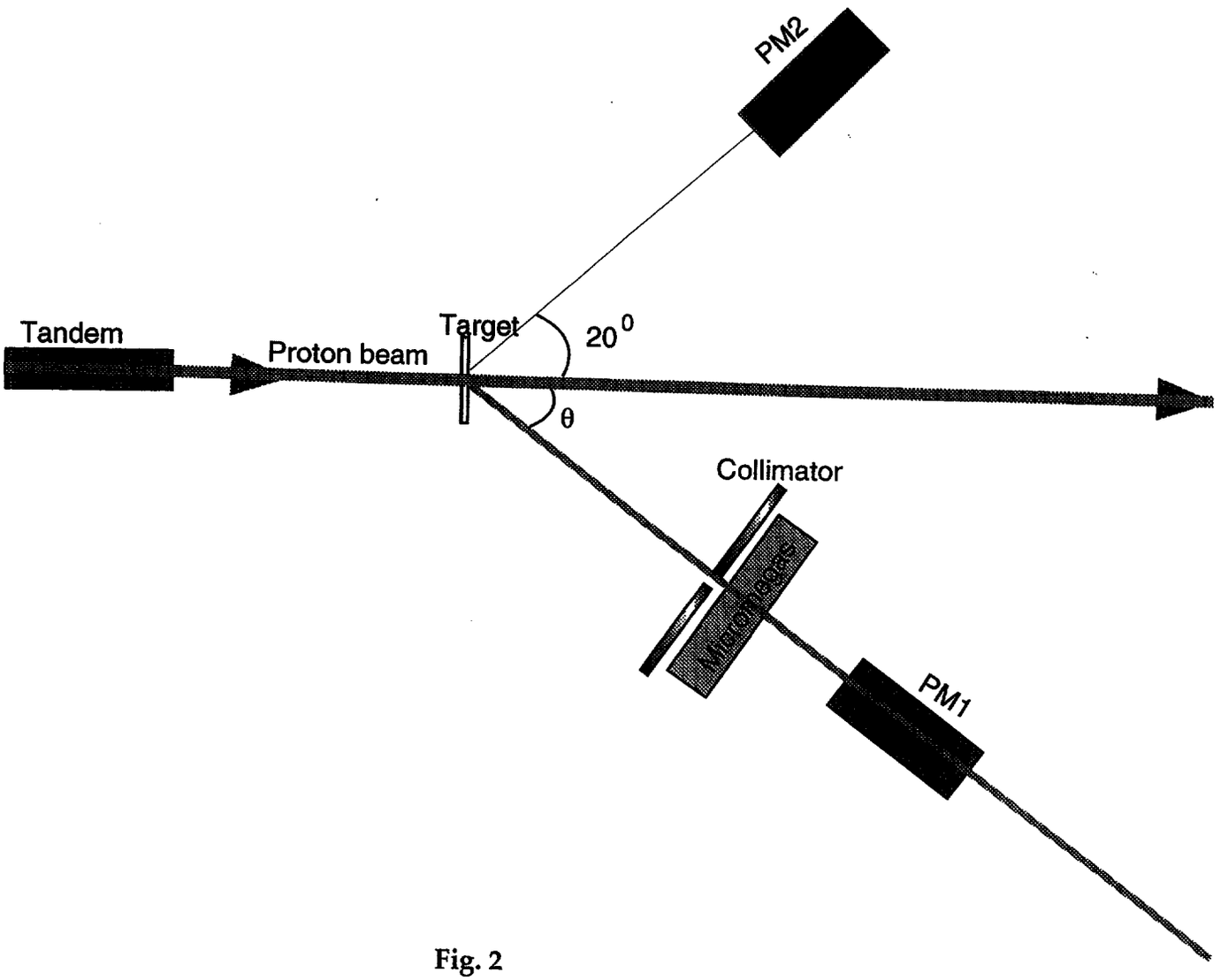

Fig. 2

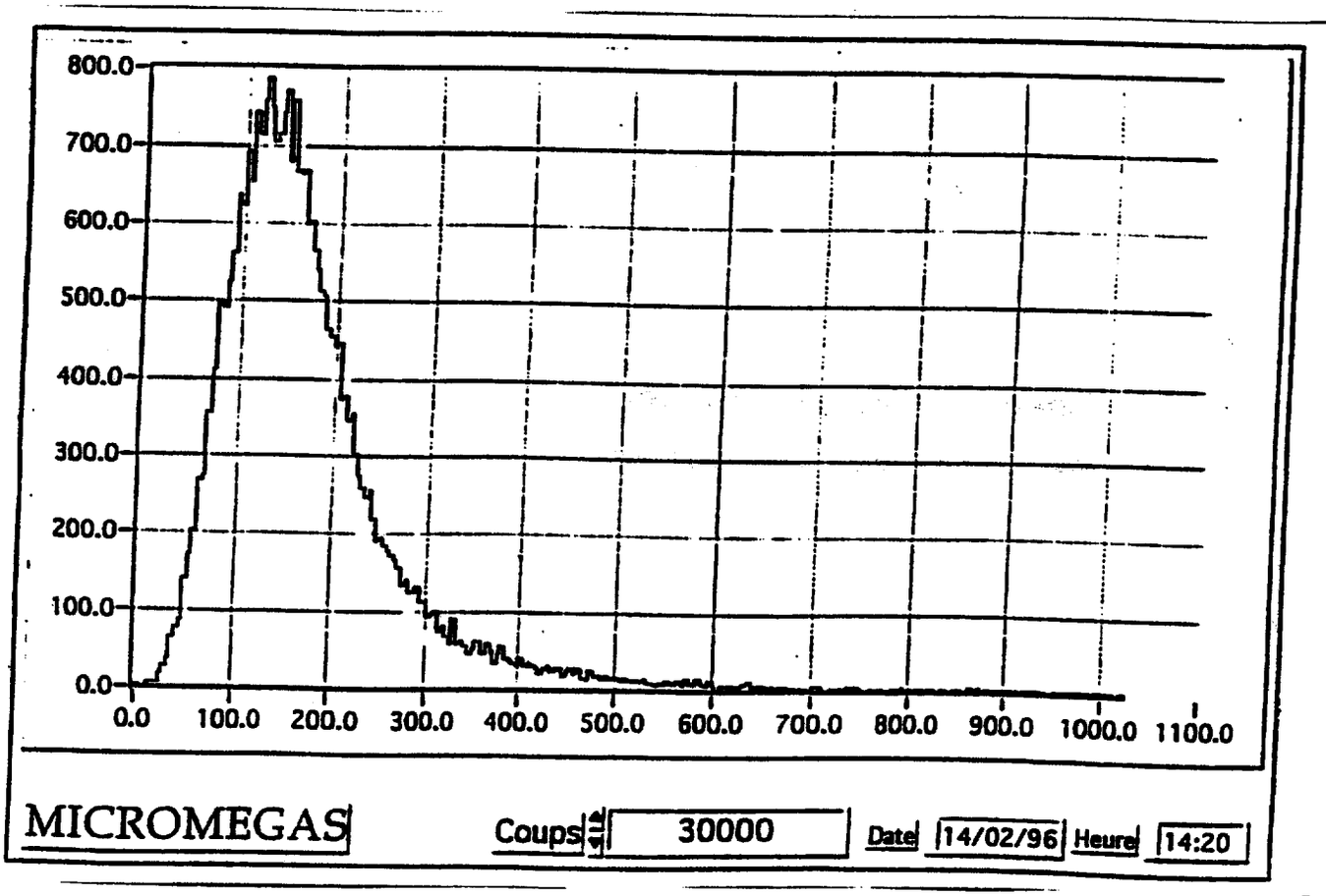
800.0
700.0
600.0
500.0
400.0
300.0
200.0
100.0
0.0
0.0 100.0 200.0 300.0 400.0 500.0 600.0 700.0 800.0 900.0 1000.0 1100.0
MICROMEGAS
Coups
30000
Date
14/02/96
Heure
14:20

Fig. 3

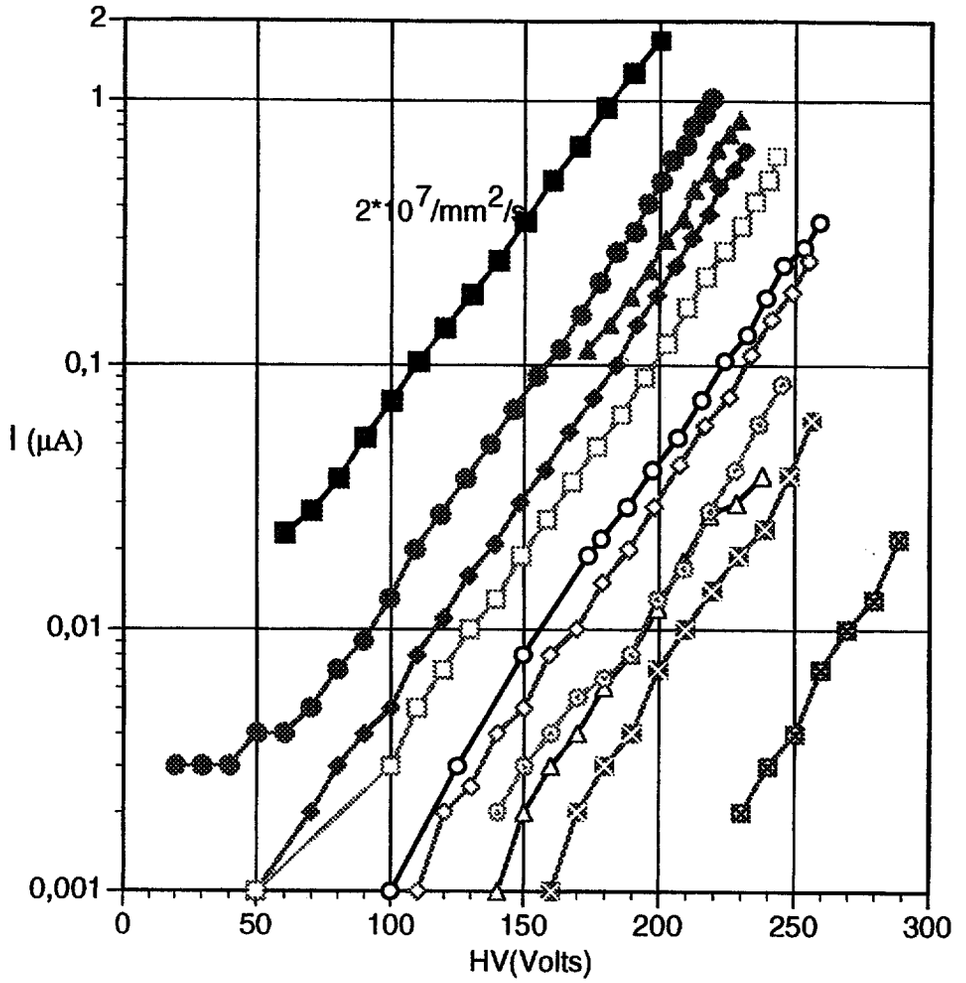

Fig. 4

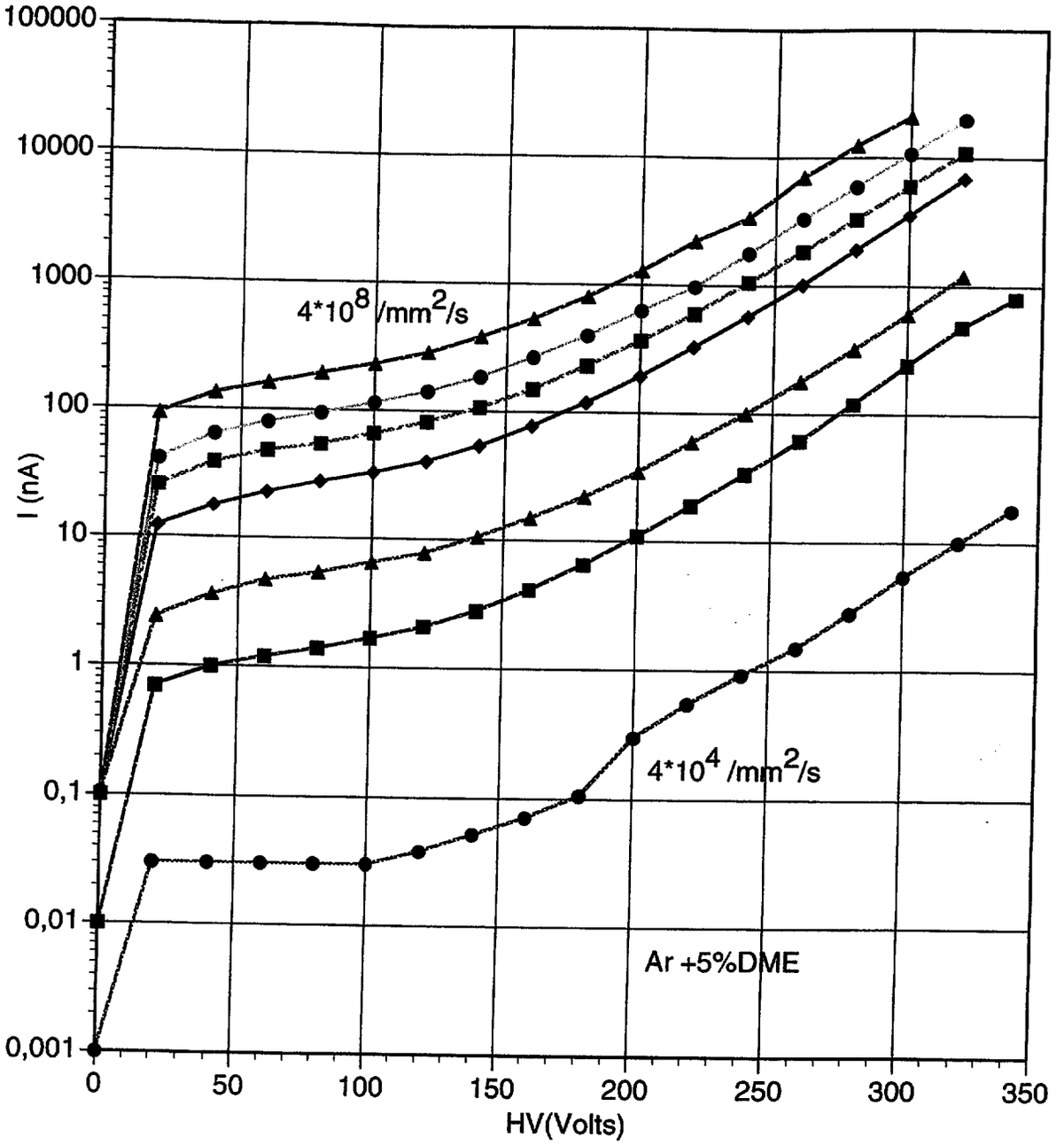
100000
10000
1000
100
10
1
0,1
0,01
0,001
I (nA)
4*10^8 /mm^2/s
4*10^4 /mm^2/s
Ar +5%DME
0
50
100
150
200
250
300
350
HV(Volts)

Fig. 5

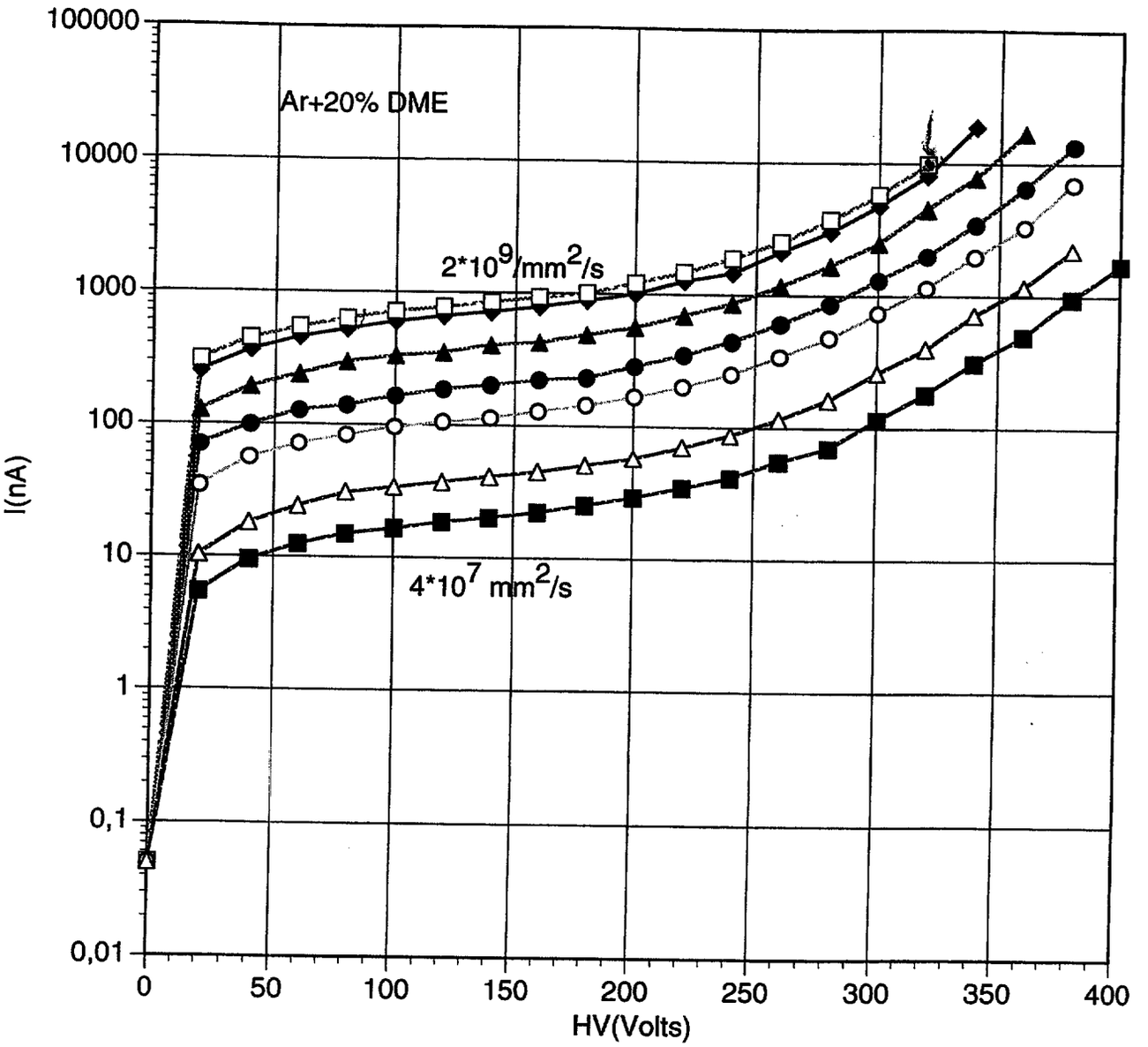
Ar+20% DME
2*10^9/mm^2/s
4*10^7 mm^2/s
I(nA)
HV(Volts)
100000
10000
1000
100
10
1
0,1
0,01
0
50
100
150
200
250
300
350
400

Fig. 6

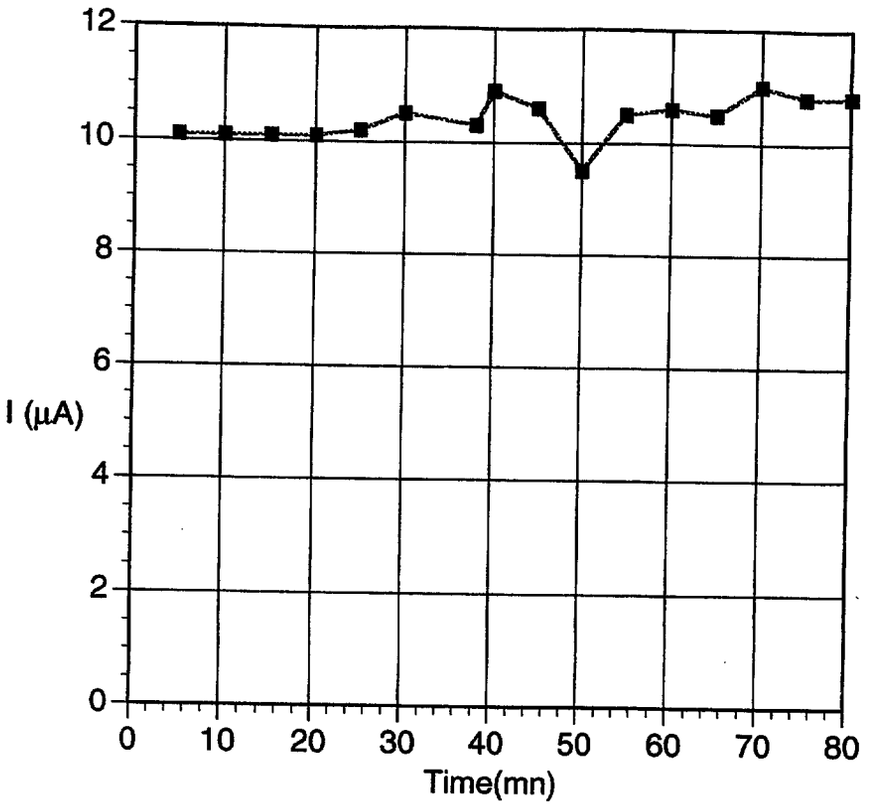

Fig. 7

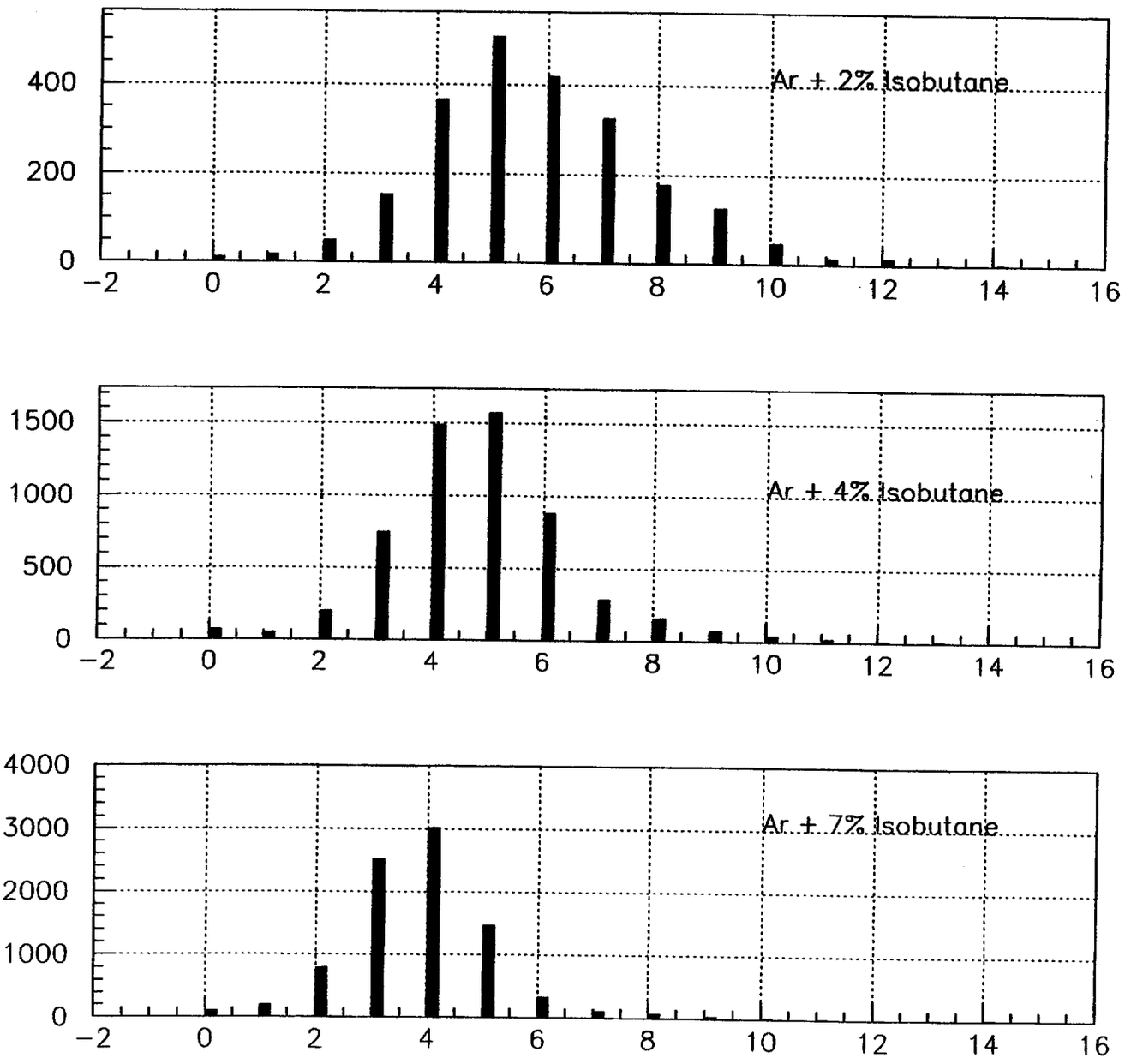

Fig. 8

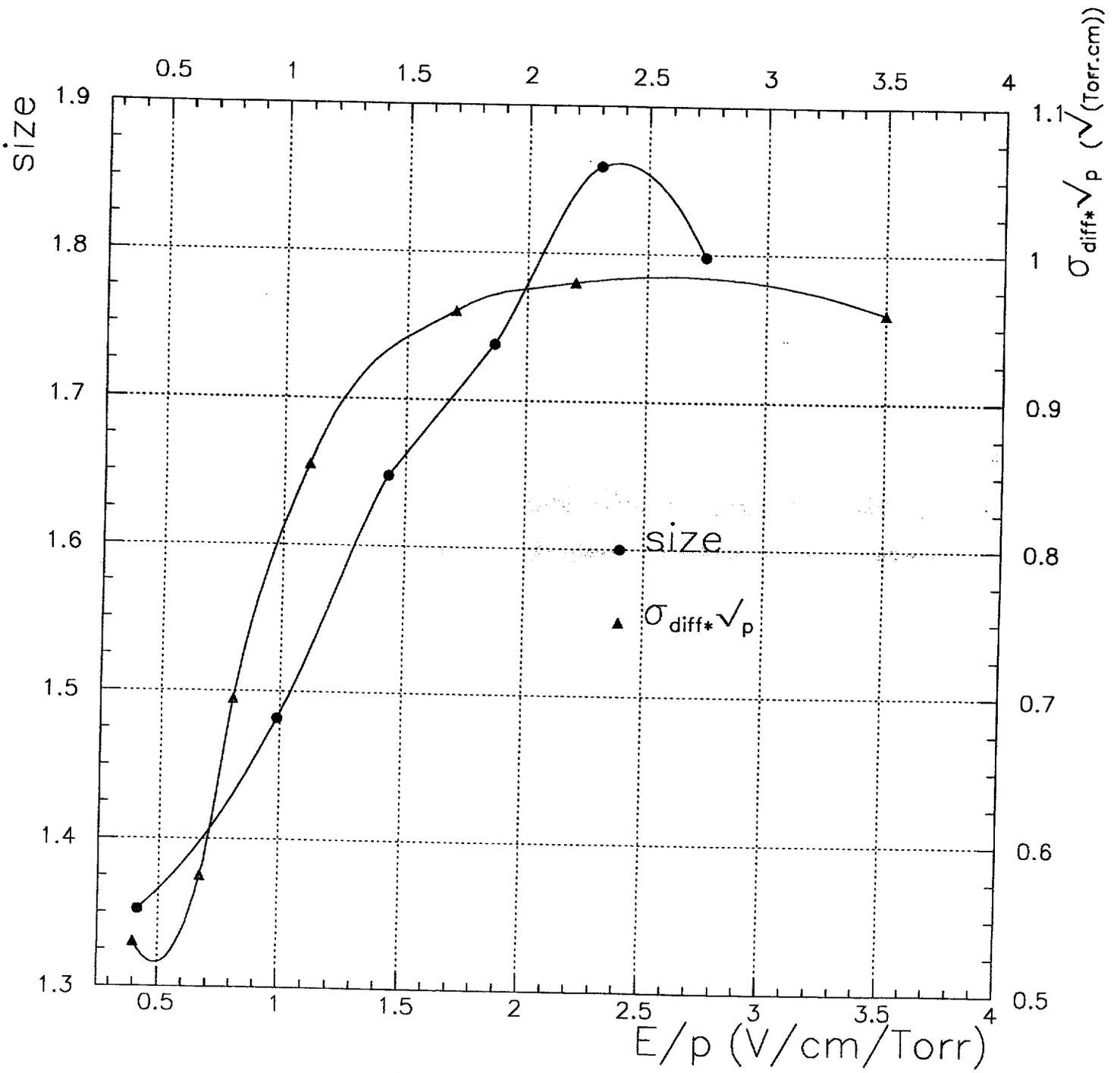
size
$\sigma_{diff*}\sqrt{p}$ ($\sqrt{(Torr.cm)}$)
E/p (V/cm/Torr)
size
$\sigma_{diff*}\sqrt{p}$
0.5
1
1.5
2
2.5
3
3.5
4
1.3
1.4
1.5
1.6
1.7
1.8
1.9
0.5
0.6
0.7
0.8
0.9
1
1.1

Fig. 9

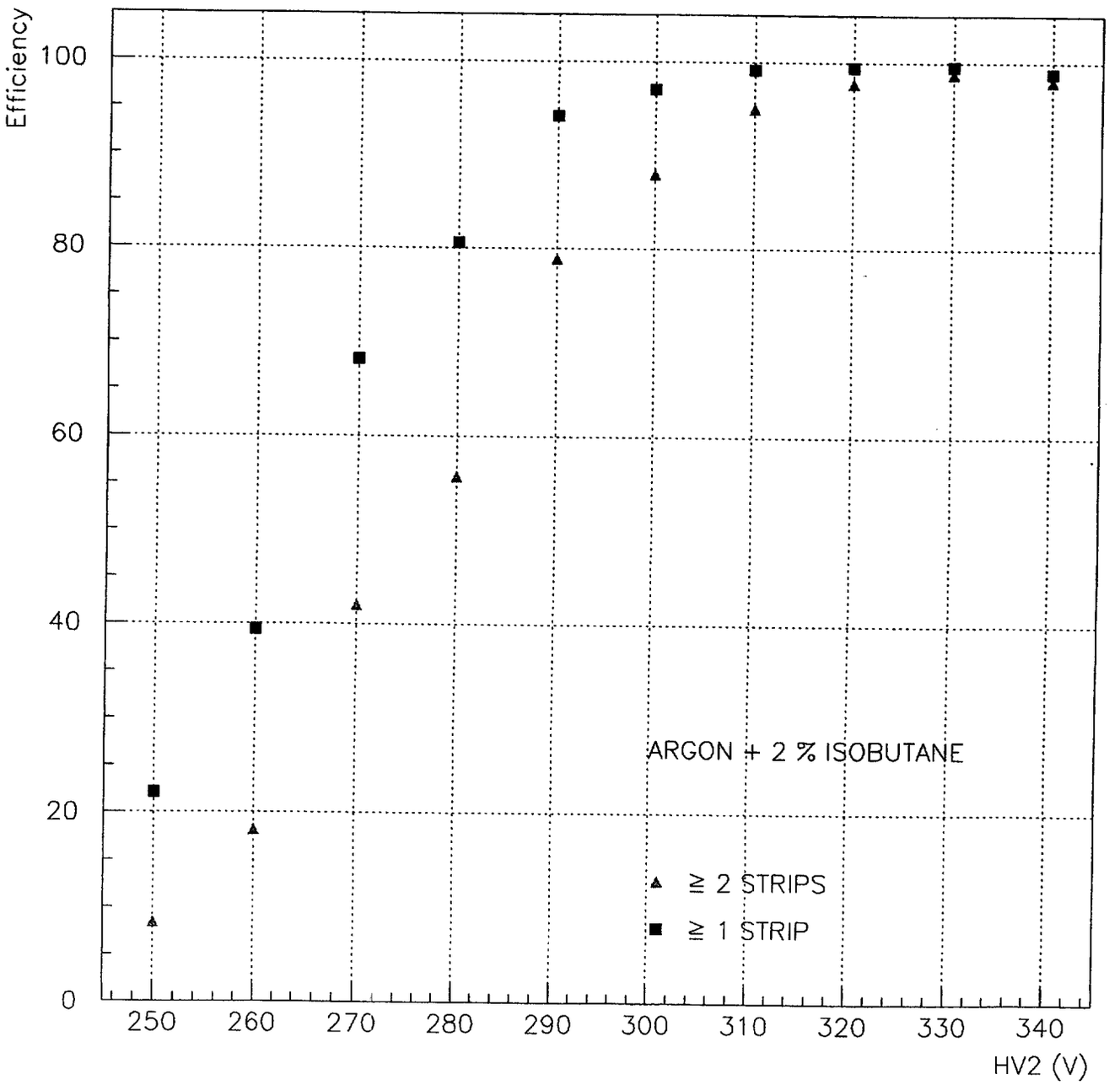
Efficiency
100
80
60
40
20
0
250
260
270
280
290
300
310
320
330
340
HV2 (V)
ARGON + 2 % ISOBUTANE
≧ 2 STRIPS
≧ 1 STRIP

Fig. 10 a)

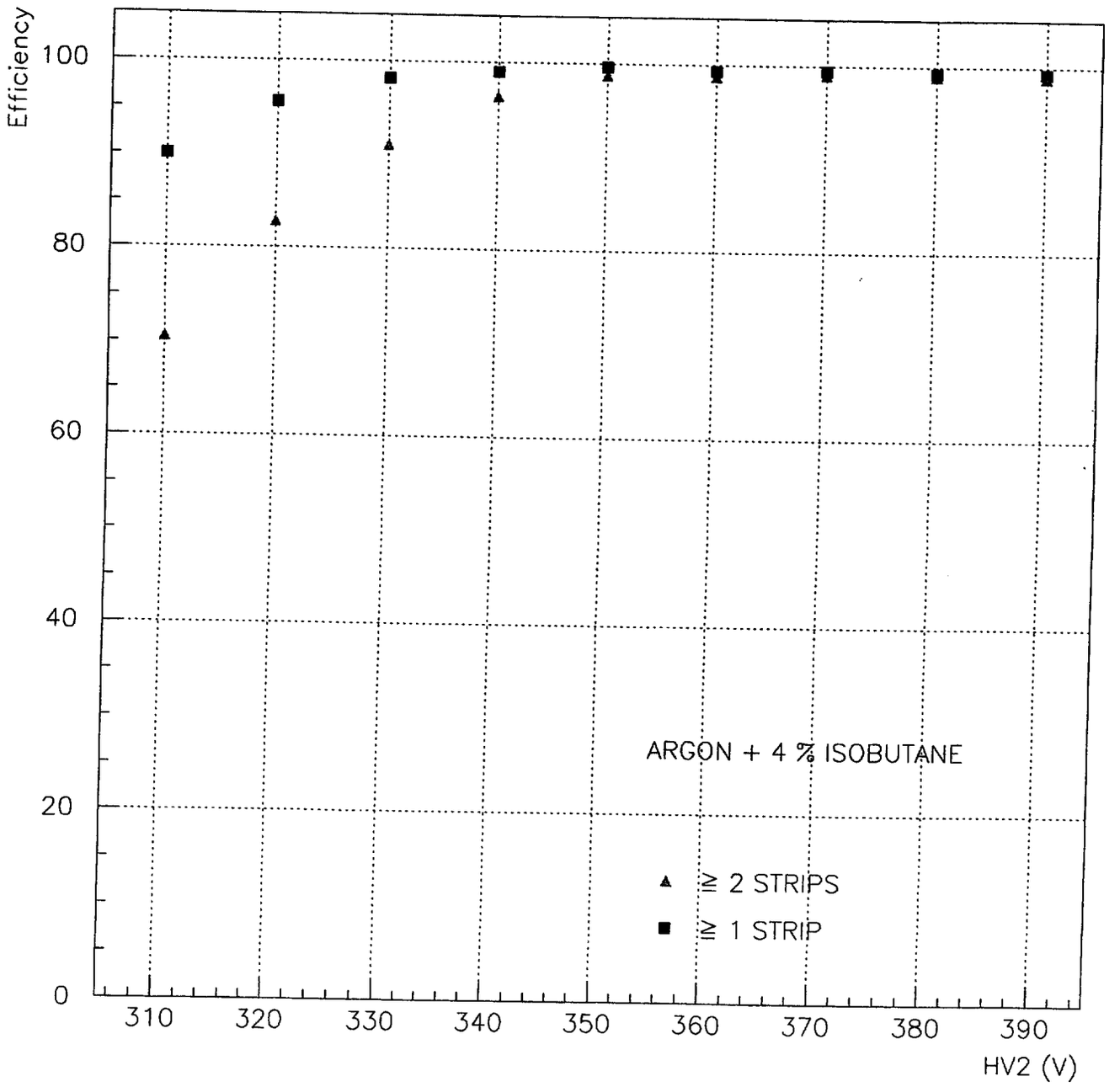
Efficiency
100
80
60
40
20
0
310
320
330
340
350
360
370
380
390
HV2 (V)
ARGON + 4 % ISOBUTANE
≧ 2 STRIPS
≧ 1 STRIP

Fig. 10 b)

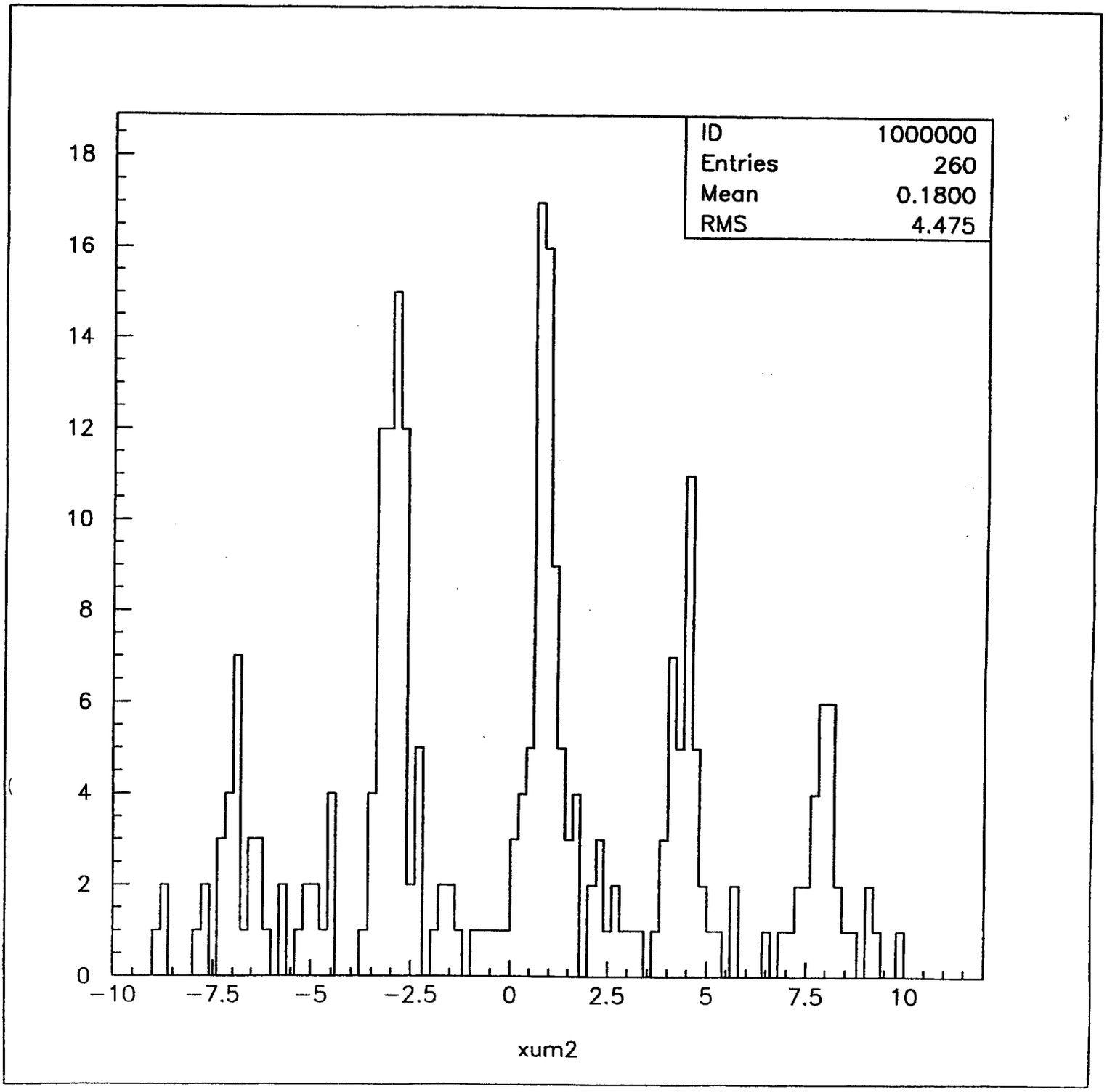
ID 1000000
Entries 260
Mean 0.1800
RMS 4.475
18
16
14
12
10
8
6
4
2
0
−10
−7.5
−5
−2.5
0
2.5
5
7.5
10
xum2

Fig. 11

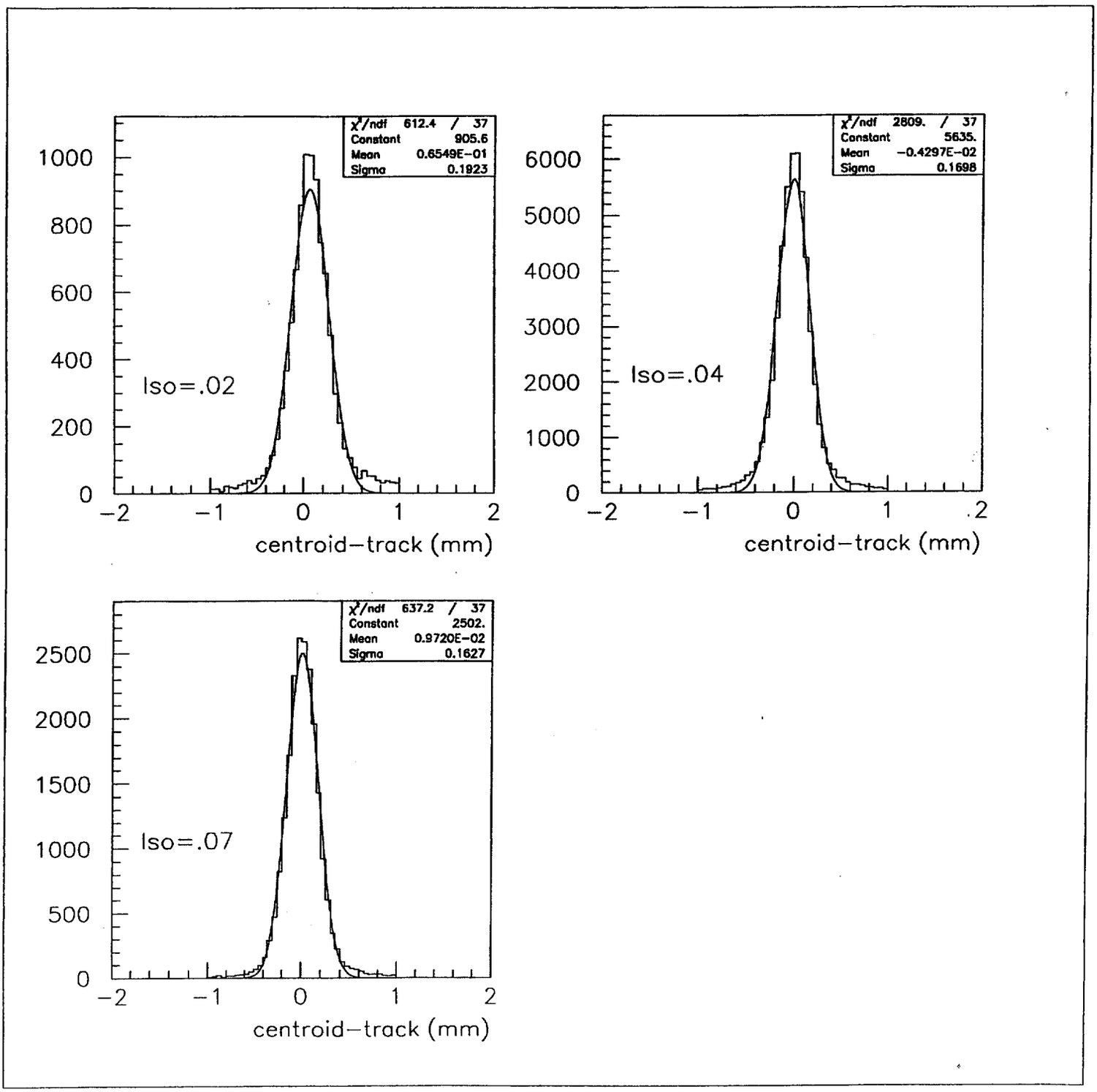
χ²/ndf 612.4 / 37
Constant 905.6
Mean 0.6549E-01
Sigma 0.1923
Iso=.02
centroid−track (mm)
χ²/ndf 2809. / 37
Constant 5635.
Mean −0.4297E-02
Sigma 0.1698
Iso=.04
centroid−track (mm)
χ²/ndf 637.2 / 37
Constant 2502.
Mean 0.9720E-02
Sigma 0.1627
Iso=.07
centroid−track (mm)

Fig. 12